Electronic Supplementary Material (ESI) for Journal of Materials Chemistry A.

Supporting Information

A Facile Soft-Template-Morphology-Controlled (STMC) Synthesis of $ZnIn_2S_4$ Nanostructures and Excellent Morphology Dependent Adsorption Properties

Afaq Ahmad Khan, Arif Chowdhury, Sunita Kumari and Sahid Hussain*

Department of Chemistry, Indian Institute of Technology Patna, Bihta, 801103

Email address: sahid@iitp.ac.in Tel: +91-612-302 8022, Fax: +91-612-2277383

Table S1 Comparison of MG adsorption on ZIS-3 with other reported materials.

S. No.	Adsorbent	pH	Q_m ($mg.g^{-1}$)	Reference
01	CO_2 -activated porous carbon	Undefined	284	1
02	r-GO	3.7	476.2	2
03	Chitosan beads	7	360	3
04	Si-POPs	6	757	4
05	Fe-Cu based adsorbent	6.58	1399	5
06.	Fe_3O_4@MgSi	4.8	125.15	6
07	TiO_2/γCD NPs	Undefined	244	7
08	Ternary Mg/(Al + Fe) Layered Double Hydroxides	4	1072.82	8
09	Magnetic phosphate nanocomposites	5	192.31	9
10	AgOH-AC nanoparticles	8	57.13	10
11	MgO/Fe_3O_4 nanoparticles	>6	4031.96	11
12	PAC/graphene nanocomposite	Undefined	1862.6	12
13	**$ZnIn_2S_4$ NS**	**4.3**	**1525**	**This work**

Table S2 Comparison of $Cr_2O_7^{2-}$ adsorption on ZIS-3 with other reported materials.

S. No.	Adsorbent	pH	Q_m (mg.g^{-1})	Reference
01	Fe_3O_4 microspheres	undefined	68.7	13
02	Magnetic carbon nanocomposite	7	3.74	14
03.	TiO_2 microspheres	2	~6.80	15
04	Bt/Bc/α-Fe_2O_3 nanoparticles	undefined	81.7	16
05	NH_2-GO/ZnO-$ZnFe_2O_4$ nanomaterials	4	109.89	17
06	Fe/C composites	5	107	18
07	Fe_3O_4-FeB nanocomposite	6.3	38.9	19
08	MnO_2	5.9	0.89	20
09	NiO nanoparticles	undefined	4.73	21
10	Zr(IV)-MOF, BUT-39	3	212	22
11	CON-LDU2	Undefined	325	23
12	CS-IL conjugation	7	91.2	24
13	**$ZnIn_2S_4$ NS**	**7**	**313**	**This work**

Table. S3 Reaction condition for preparation of $ZnIn_2S_4$ NS

S. No.	Sample Name	Sulfur source (5 mmol)	Soft-template (Surfactant)	Temp & Time (min)	mmol	
					$In(OAc)_3$	$Zn(OAc)_2.2H_2O$
1.	ZIS-1	Thiourea	Glycerol	150°C, 180	1	1
3.	ZIS-2		PEG-200			
4.	ZIS-3		PEG-PPG-PEG			

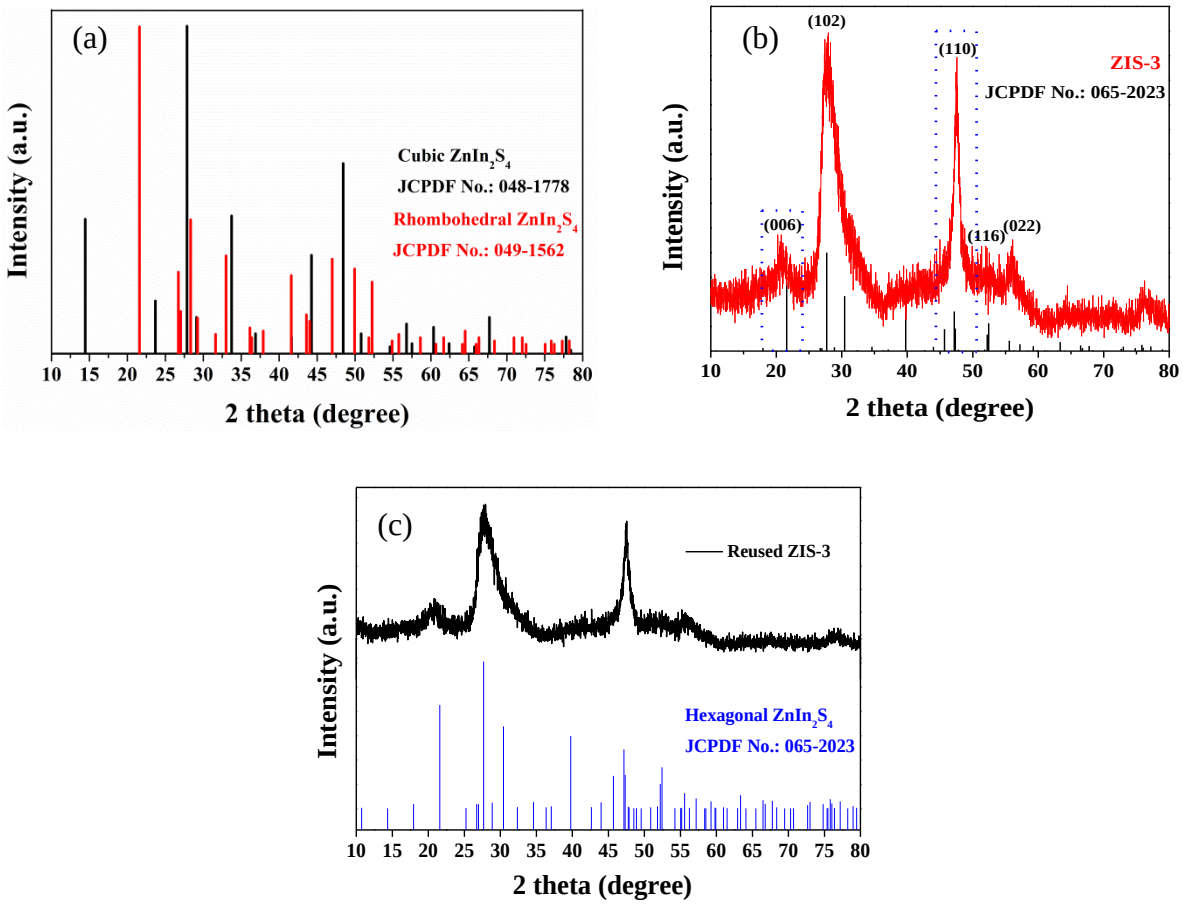

Fig. S1 P-XRD pattern of standard cubic and rhombohedral $ZnIn_2S_4$ (a), P-XRD of ZIS-3 with standard hexagonal $ZnIn_2S_4$ (b) and reused ZIS-3 (c).

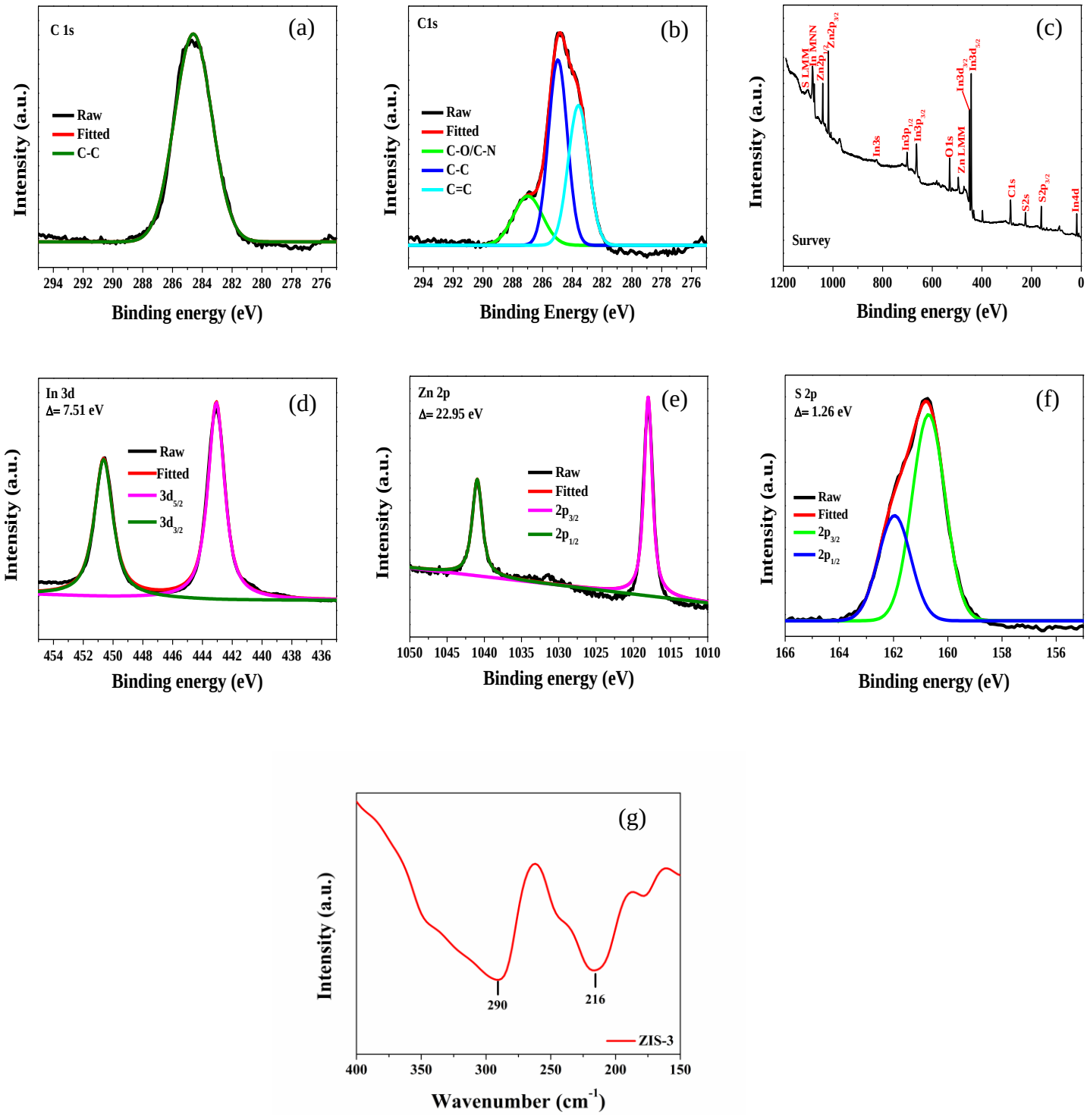

Fig. S2 XPS spectra; C1s spectra of ZIS-1 (a), C1s spectra (b), survey spectra (c), core-level In3d spectra (d), core-level Zn 2p spectra (e), core-level S2p spectra (f), of reused ZIS-3 and far-IR spectra of ZIS-3 (g).

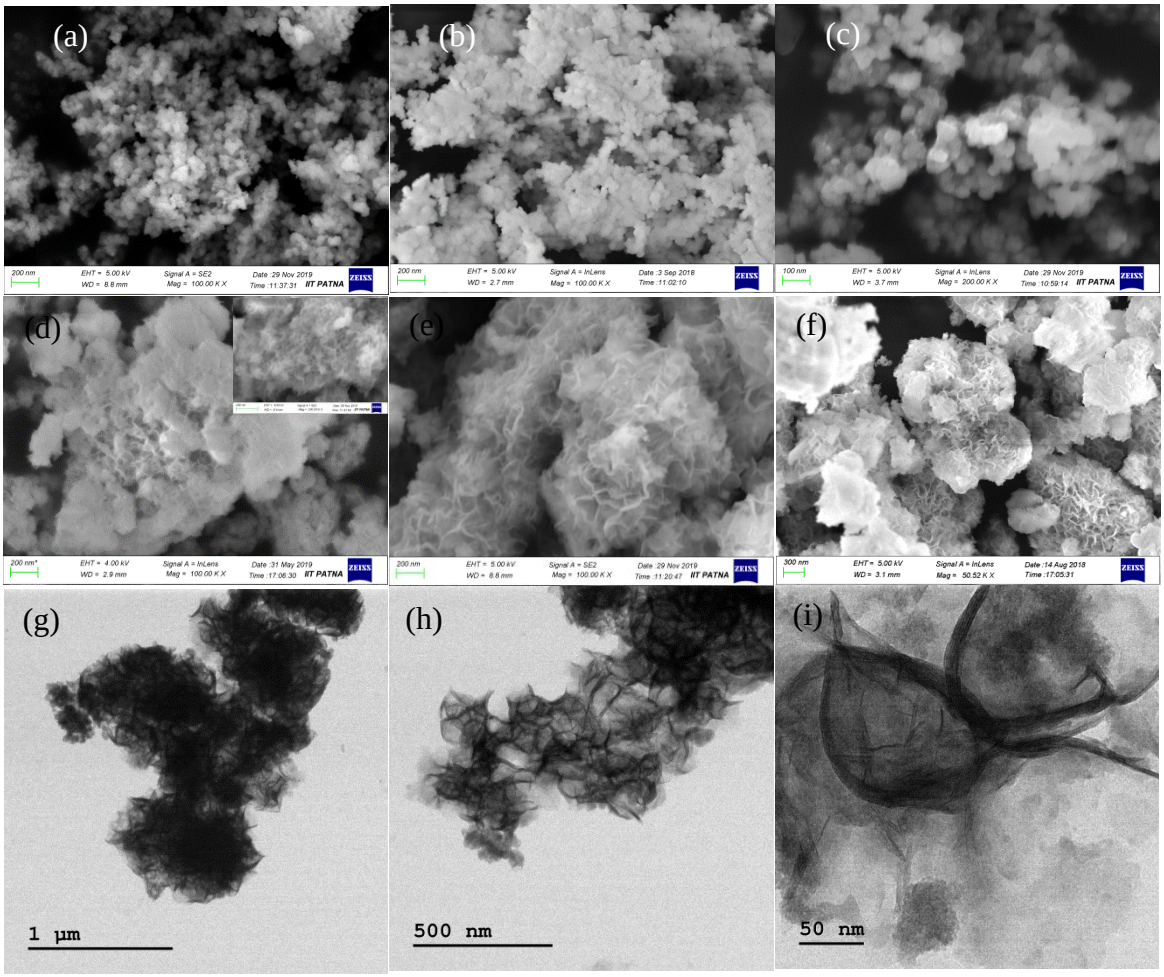

Fig. S3 FE-SEM micrograph: SE2 mode at 100K magnification (a), InLens mode at 100K magnification (b), InLens mode at 200K magnification (c) of ZIS-1; InLens mode at 100K inset with SE2 mode at 200K magnification (d) of ZIS-2; SE2 mode at 100K magnification (e), InLens mode at 50.52K magnification (f) of ZIS-3; TEM micrograph of ZIS-3 (g-i).

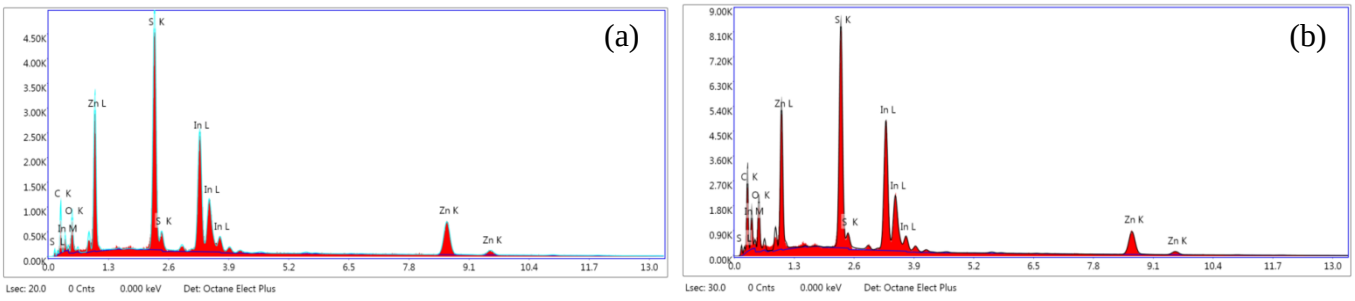

Fig. S4 EDS line spectra of ZIS-1 (a) and ZIS-2 (b).

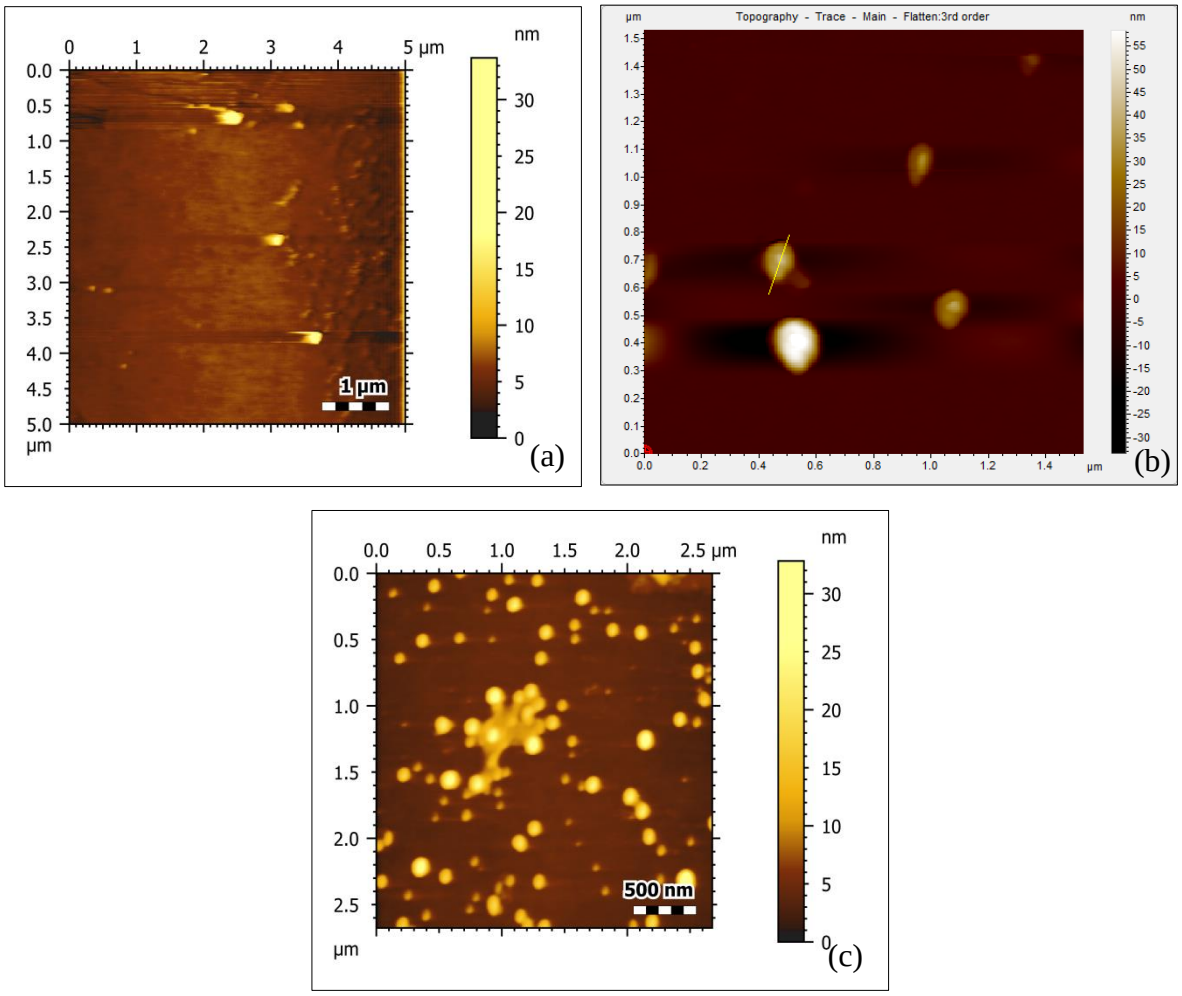

Fig. S5 AFM topography of the ZIS-1 (a), ZIS-2 (b) and ZIS-3 (c).

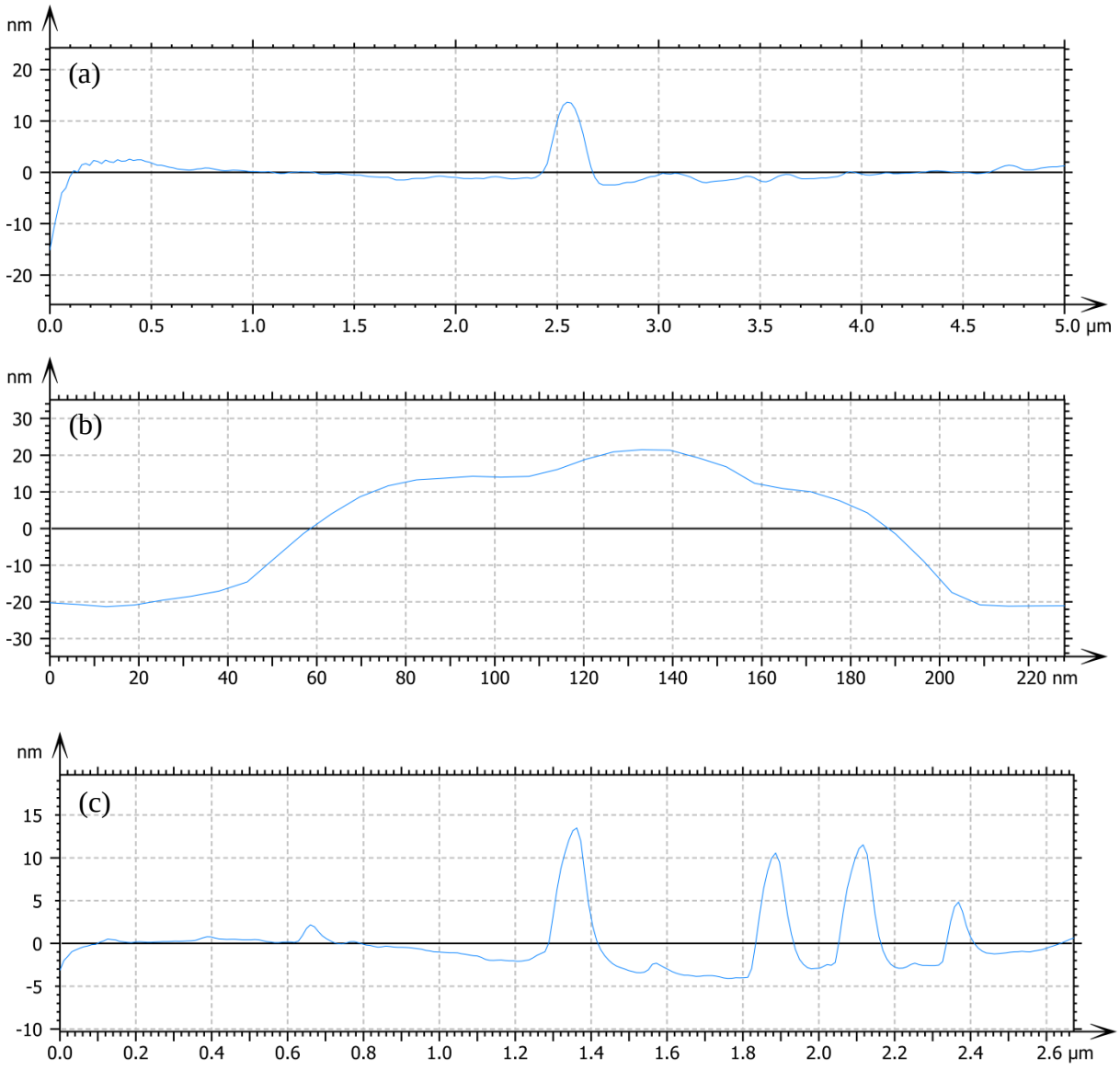

Fig. S6 Thickness profile curve of the ZIS-1 (a), ZIS-2 (b) and ZIS-3 (c).

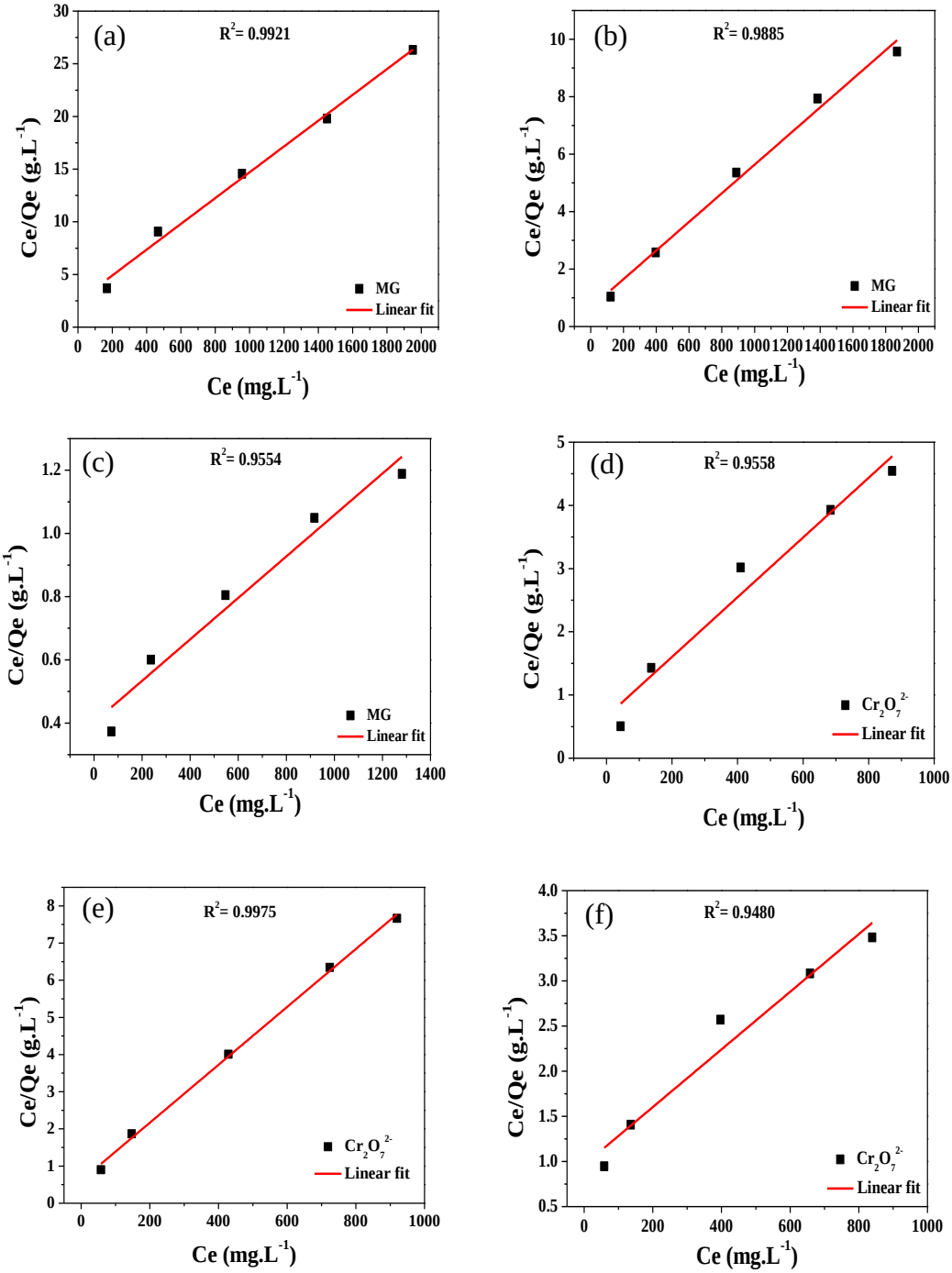

Fig. S7 Fitted Langmuir adsorption isotherm model of ZIS-1 (a), ZIS-2 (b), ZIS-3 (c) for MG adsorption and ZIS-1 (d), ZIS-2 (e), ZIS-3 (f) for the adsorption of $Cr_2O_7^{2-}$.

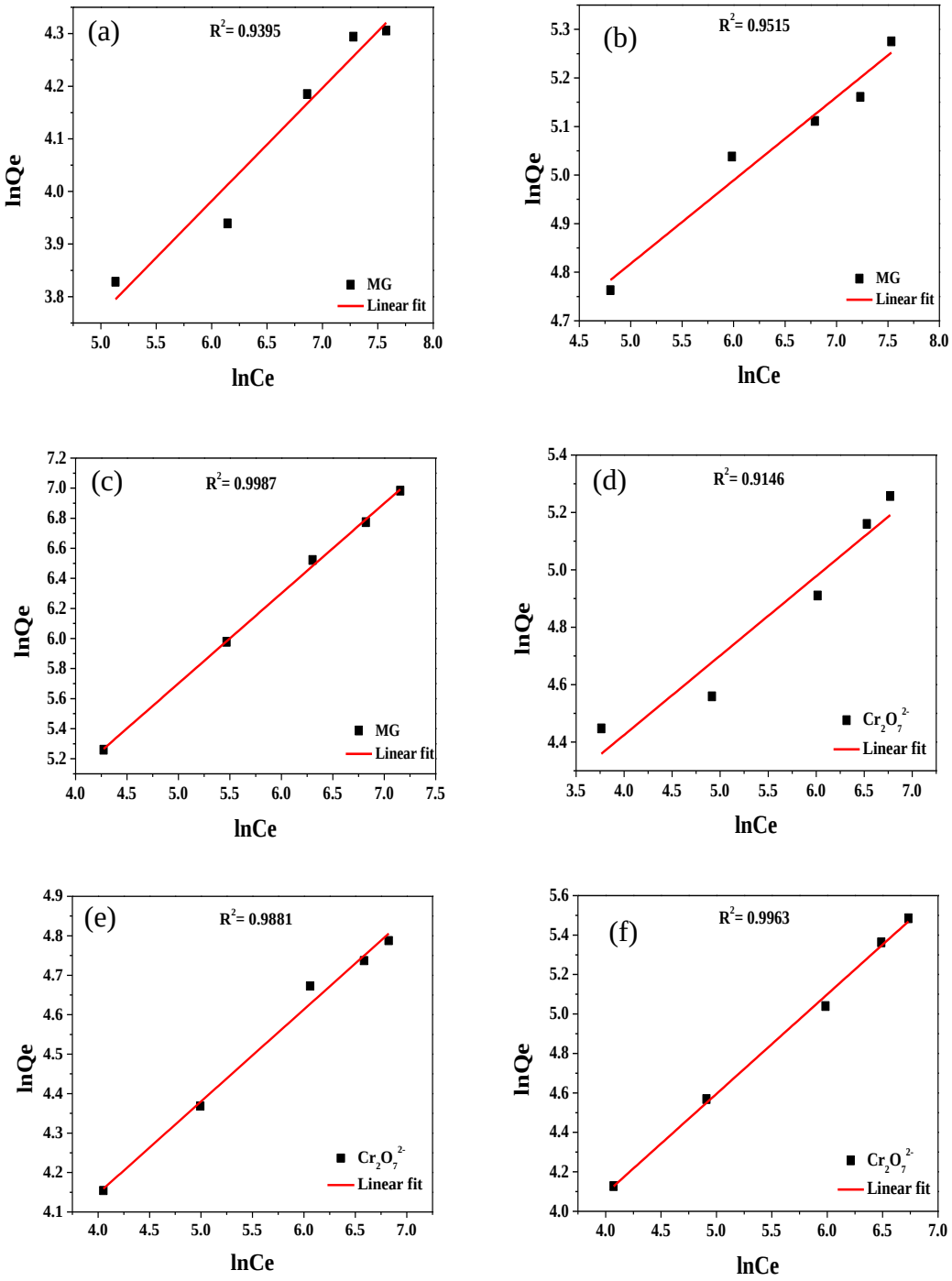

Fig. S8 Fitted Freundlich adsorption isotherm model of ZIS-1 (a), ZIS-2 (b), ZIS-3 (c) for the MG adsorption and ZIS-1 (d), ZIS-2 (e), ZIS-3 (f) for the adsorption of $Cr_2O_7^{2-}$.

Table S4 Separation factor (R_L) of MG adsorption on $ZnIn_2S_4$ NS.

Adsorbent	**R_L**				
	MG concentration ($mg.L^{-1}$)				
	200	**500**	**1000**	**1500**	**2000**
ZIS-1	0.5013	0.2868	0.1674	0.1182	0.0913
ZIS-2	0.3959	0.2077	0.1159	0.0803	0.0615
ZIS-3	0.7542	0.5511	0.3803	0.2904	0.2348

Table S5 Separation factor (R_L) of $Cr_2O_7^{2-}$ adsorption on $ZnIn_2S_4$ NS.

Adsorbent	**R_L**				
	$Cr_2O_7^{2-}$ concentration ($mg.L^{-1}$)				
	100	**200**	**500**	**800**	**1000**
ZIS-1	0.5824	0.4108	0.2181	0.1484	0.1224
ZIS-2	0.4388	0.2811	0.1352	0.0890	0.0725
ZIS-3	0.7713	0.6017	0.3767	0.2742	0.2321

Table S6 Kinetic parameters of the adsorption of MG dyes on $ZnIn_2S_4$ NS

Pseudo-first-order model						**Pseudo-second-order model**		
Adsorbent	**Conc. ($mg.L^{-1}$)**	**$q_{e,exp}$ ($mg.g^{-1}$)**	**K_1**	**$q_{e,cal}$ ($mg.g^{-1}$)**	**R^2**	**K_2**	**$q_{e,cal}$ ($mg.g^{-1}$)**	**R^2**
ZIS-1	50	17.89	0.0068	12.14	0.9477	0.0028	17.42	0.9806
	100	30.15	0.0071	19.55	0.7888	0.0017	28.92	0.9633
ZIS-2	50	49.73	0.0123	41.83	0.9403	0.0007	51.57	0.9701
	100	60.39	0.0096	39.76	0.9303	0.0011	60.31	0.9913
ZIS-3	50	74.99	0.0656	8.09	0.7664	0.0505	75	1
	100	124.65	0.0114	43.62	0.8477	0.0014	125	0.9988

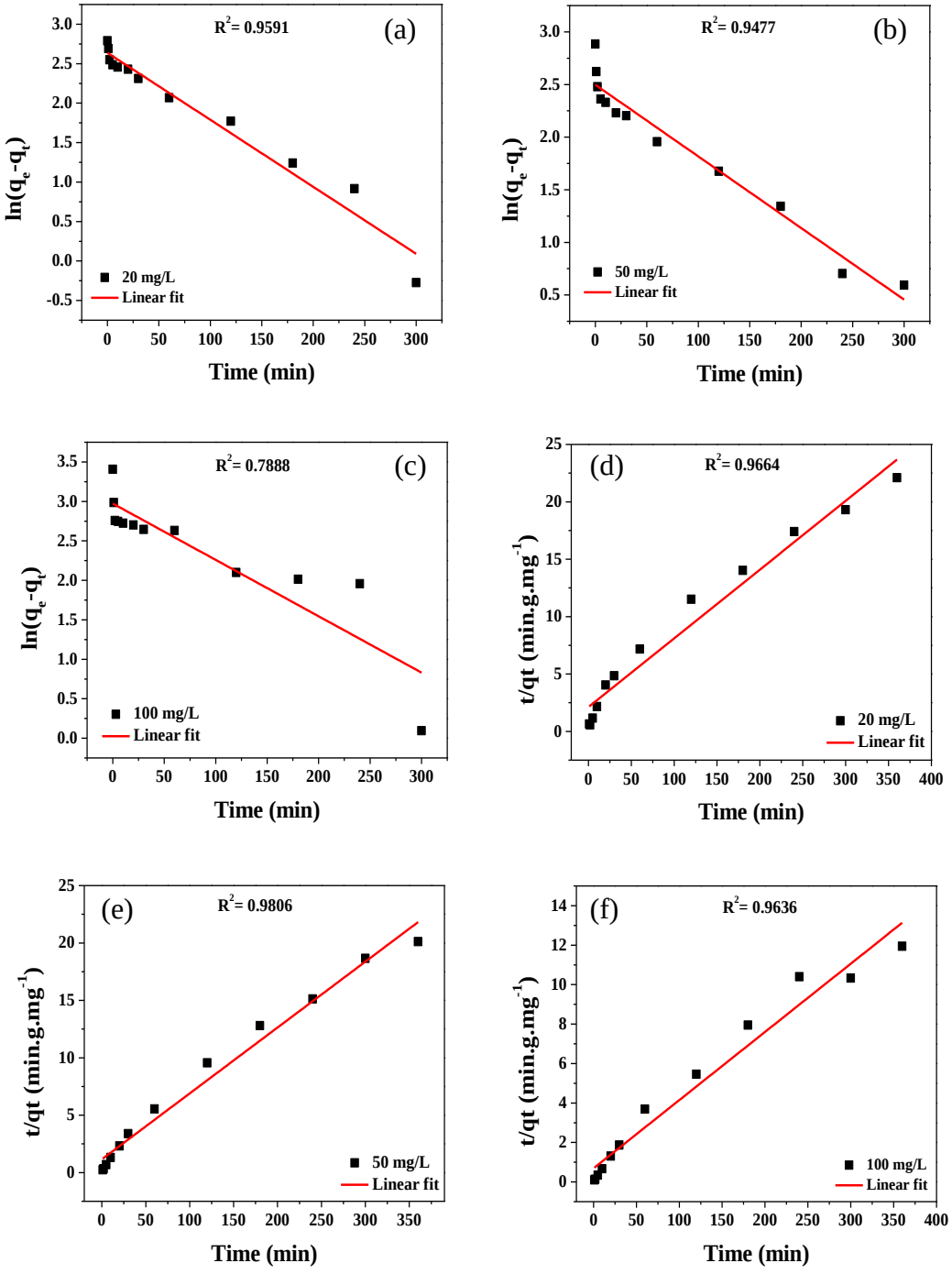

Fig. S9 Fitted pseudo-first order kinetic rate model of MG 20 mg/L (a), MG 50 mg/L (b), MG 100 mg/L (c) and fitted pseudo-second order kinetic rate model of MG 20 mg/L (d), MG 50 mg/L (e), MG 100 mg/L (f) in the presence of ZIS-1.

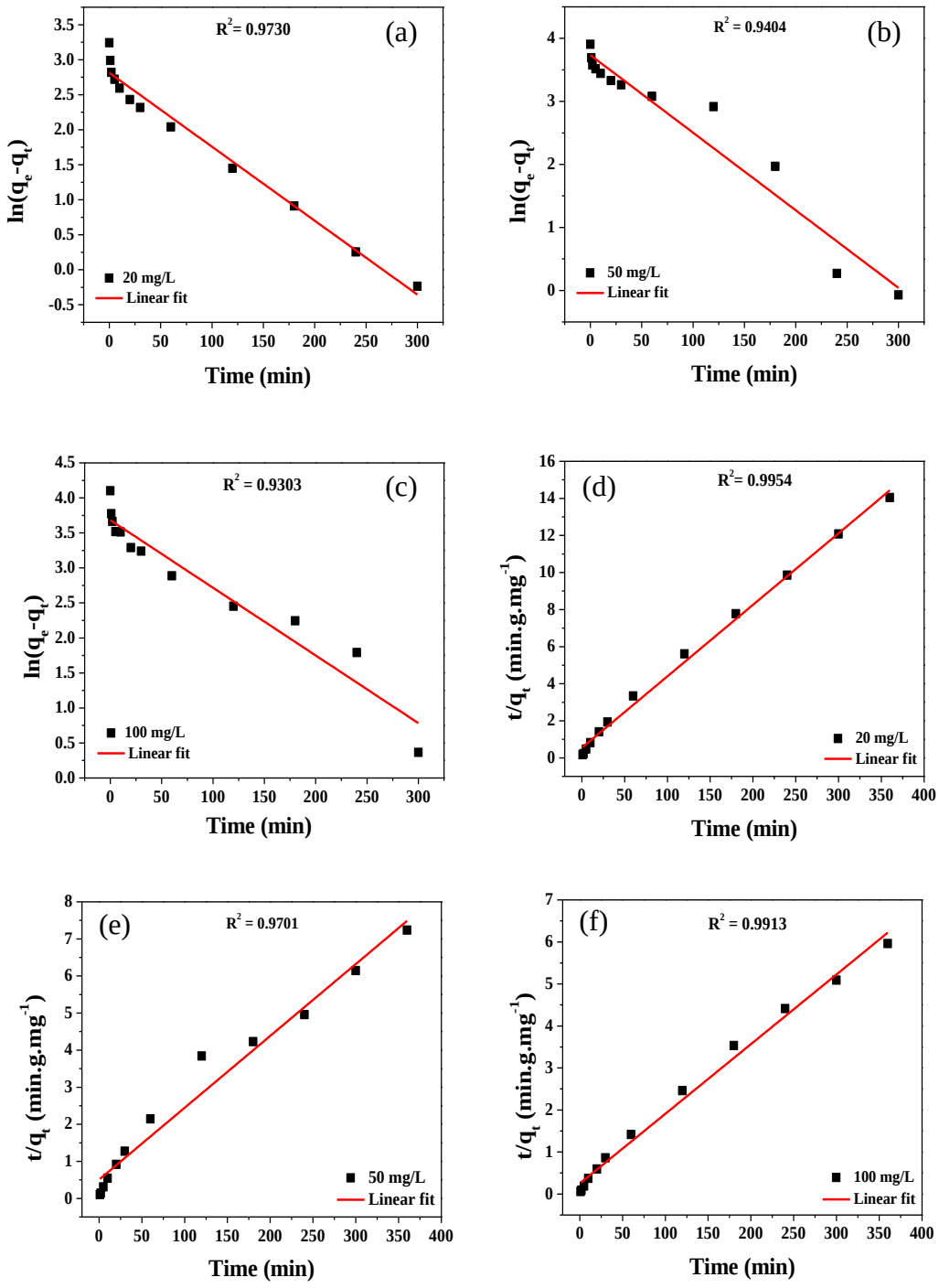

Fig. S10 Fitted pseudo-first order kinetic rate model of MG 20 mg/L (a), MG 50 mg/L (b), MG 100 mg/L (c) and fitted pseudo-second order kinetic rate model of MG 20 mg/L (d), MG 50 mg/L (e), MG 100 mg/L (f) in the presence of ZIS-2.

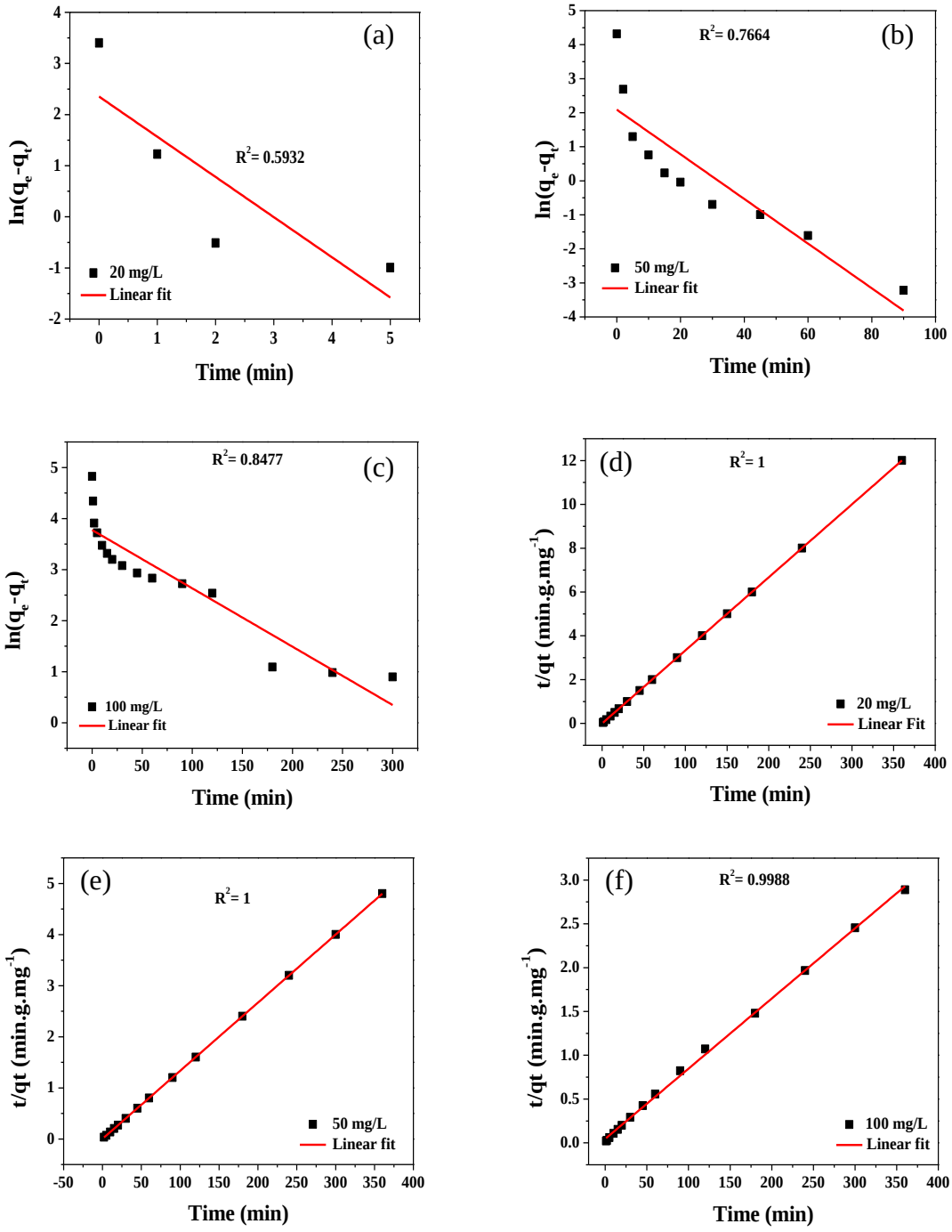

Fig. S11 Fitted pseudo-first order kinetic rate model of MG 20 mg/L (a), MG 50 mg/L (b), MG 100 mg/L (c) and fitted pseudo-second order kinetic rate model of MG 20 mg/L (d), MG 50 mg/L (e), MG 100 mg/L (f) in the presence of ZIS-3.

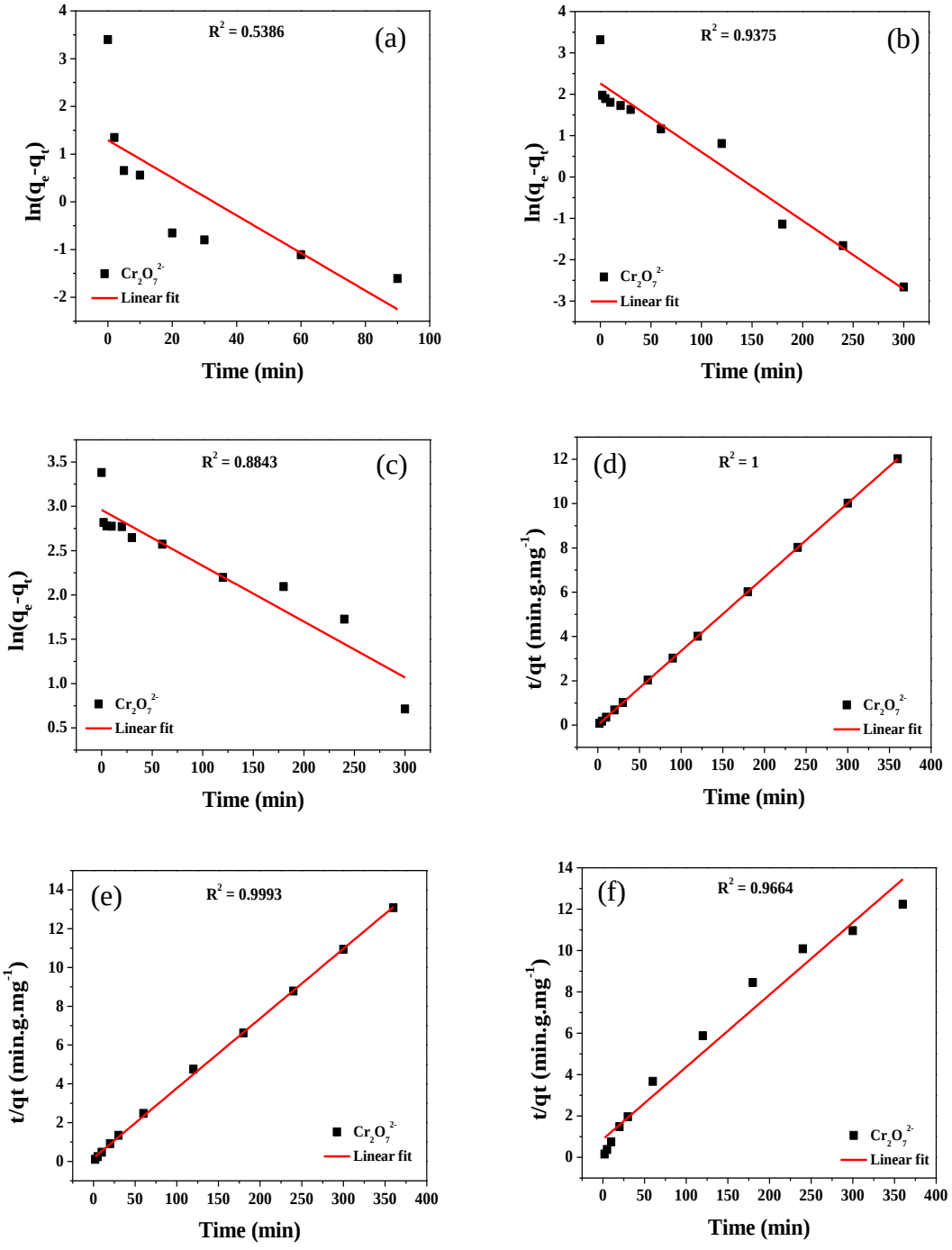

Fig. S12 Fitted pseudo-first order kinetic rate model of ZIS-1 (a), ZIS-2 (b), ZIS-3 (c) and fitted pseudo-first order kinetic rate model of ZIS-1 (d), ZIS-2 (e), ZIS-3 (f)using 20 mg.L^{-1} solution of $Cr_2O_7^{2-}$.

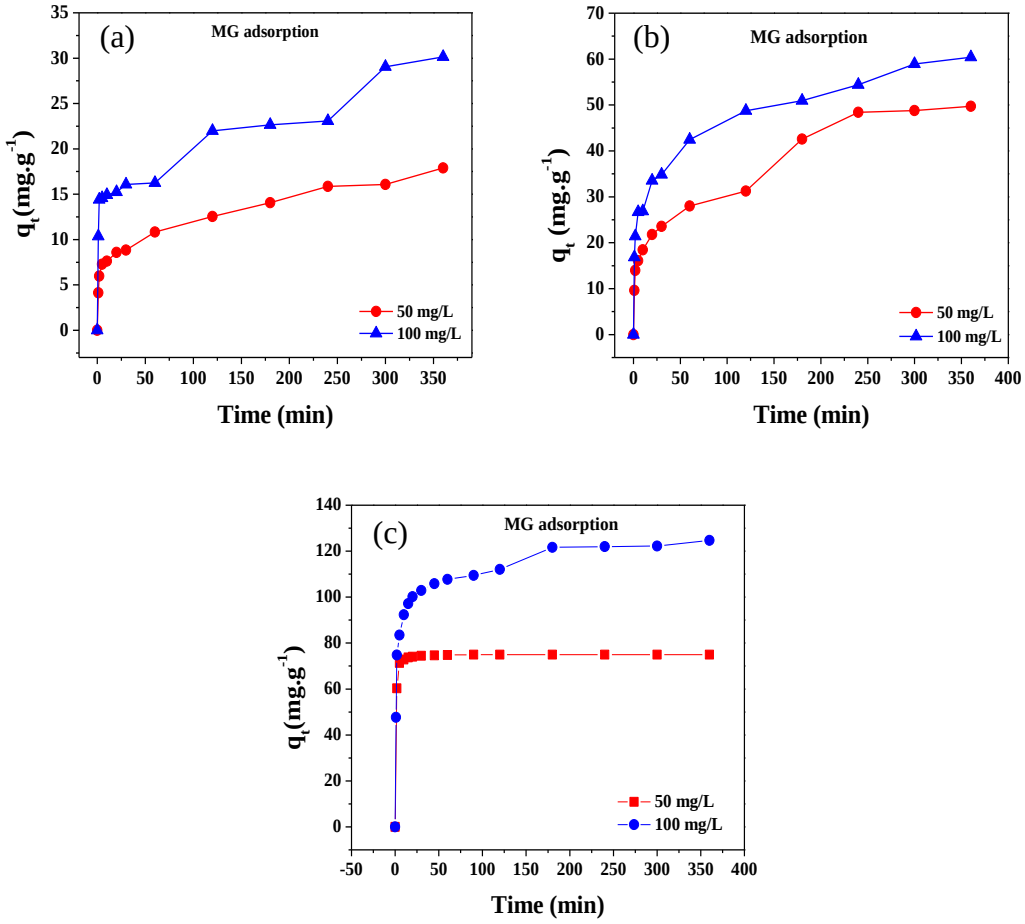

Fig. S13 Effect of contact time on the adsorption of MG using ZIS-1 (a), ZIS-2 (b), and ZIS-3 (c) at the solution concentration of 50 mg.L^{-1} and 100 mg.L^{-1}.

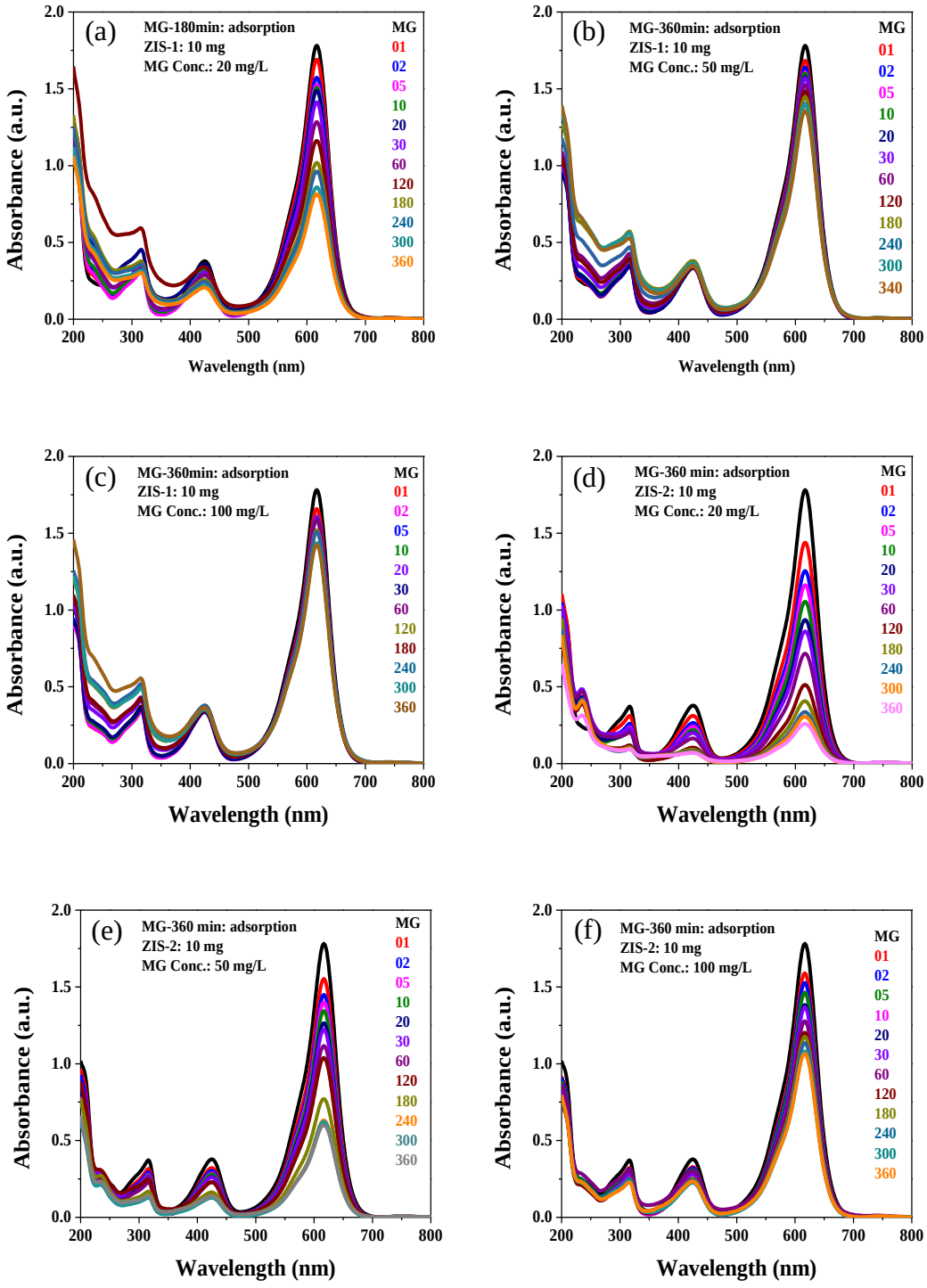

Fig. S14 UV-Vis spectra of adsorption of MG at 20 mg/L (a), 50 mg/L (b), 100 mg/L (c) using ZIS-1 and MG adsorption at 20 mg/L (d), 50 mg/L (e), 100 mg/L (f) using ZIS-2.

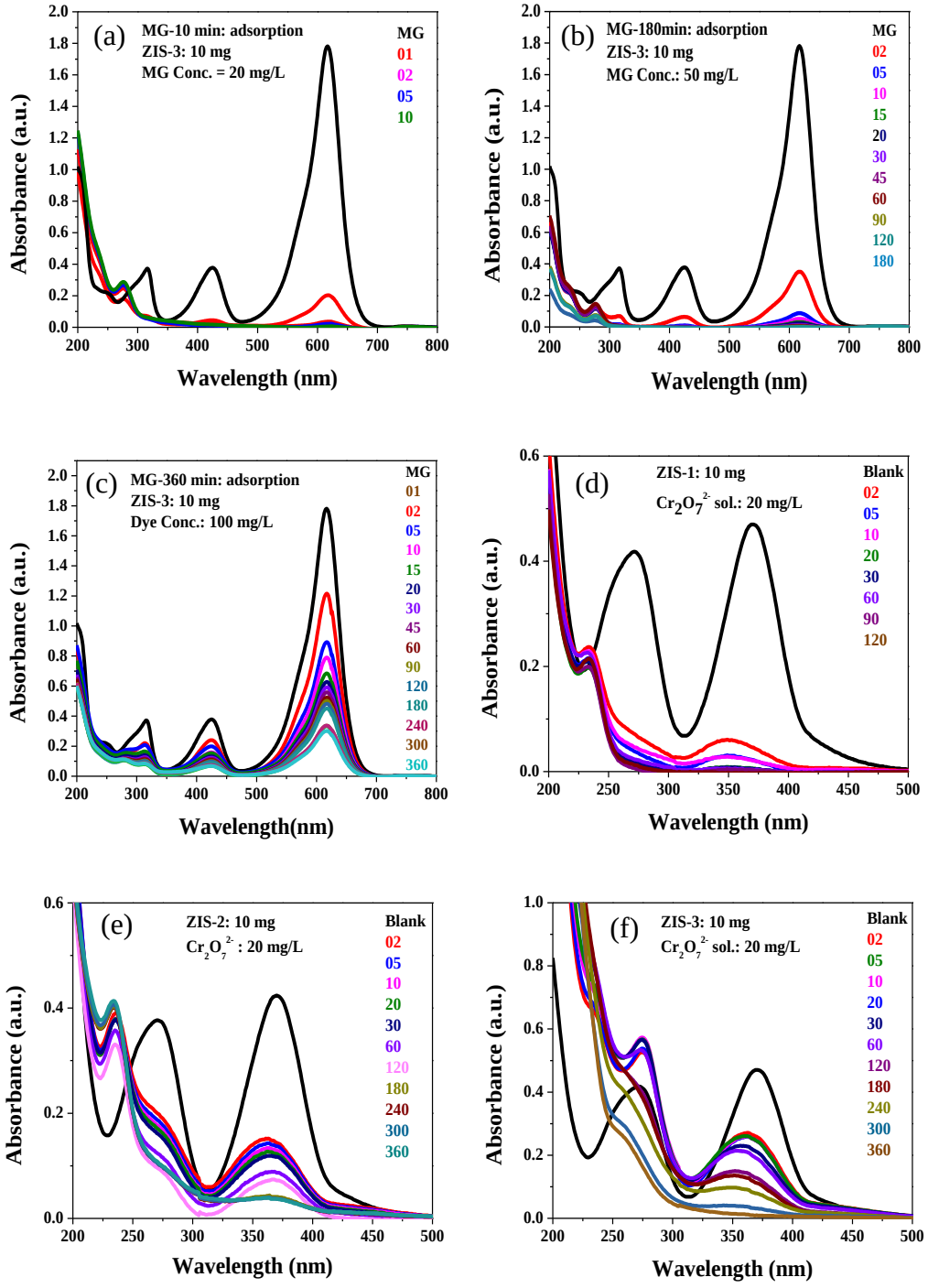

Fig. S15 UV-Vis spectra of adsorption of MG at 20 mg/L (a), 50 mg/L (b), 100 mg/L (c) using ZIS-3 and $Cr_2O_7^{2-}$ adsorption using ZIS-1 (d), ZIS-2 (e) and ZIS-3 (f) at 20 mg/L solution.

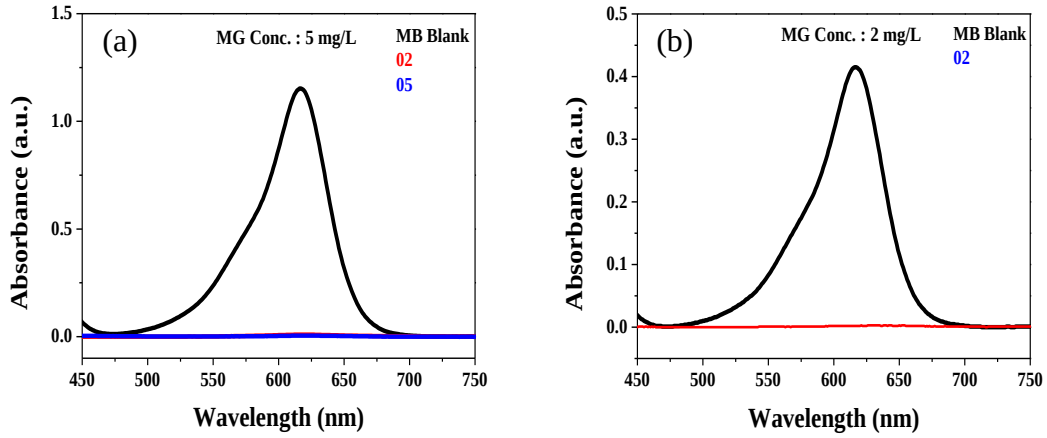

Fig. S16 UV-Vis spectra of adsorption of MG at 5 mg/L (a) and 2 mg/L (b) using ZIS-3

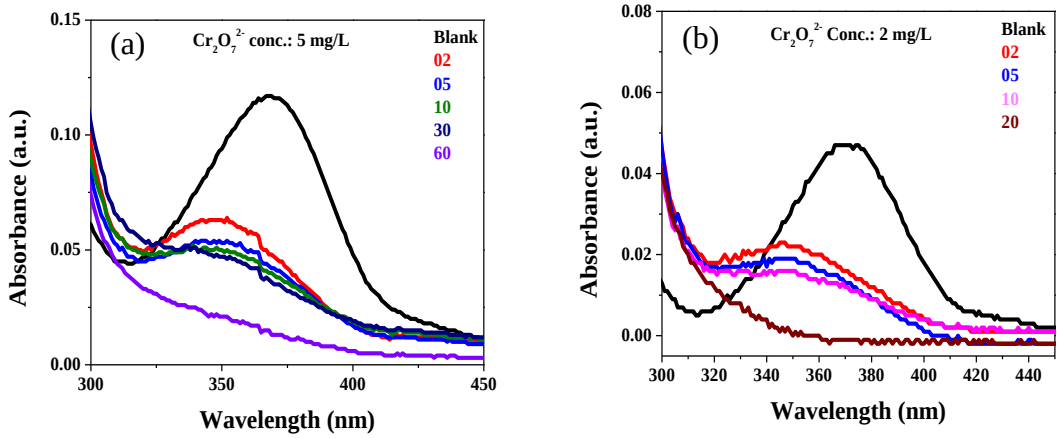

Fig. S17 UV-Vis spectra of adsorption of $Cr_2O_7^{2-}$ at 5 mg/L (a) 2 mg/L (b) using ZIS-3.

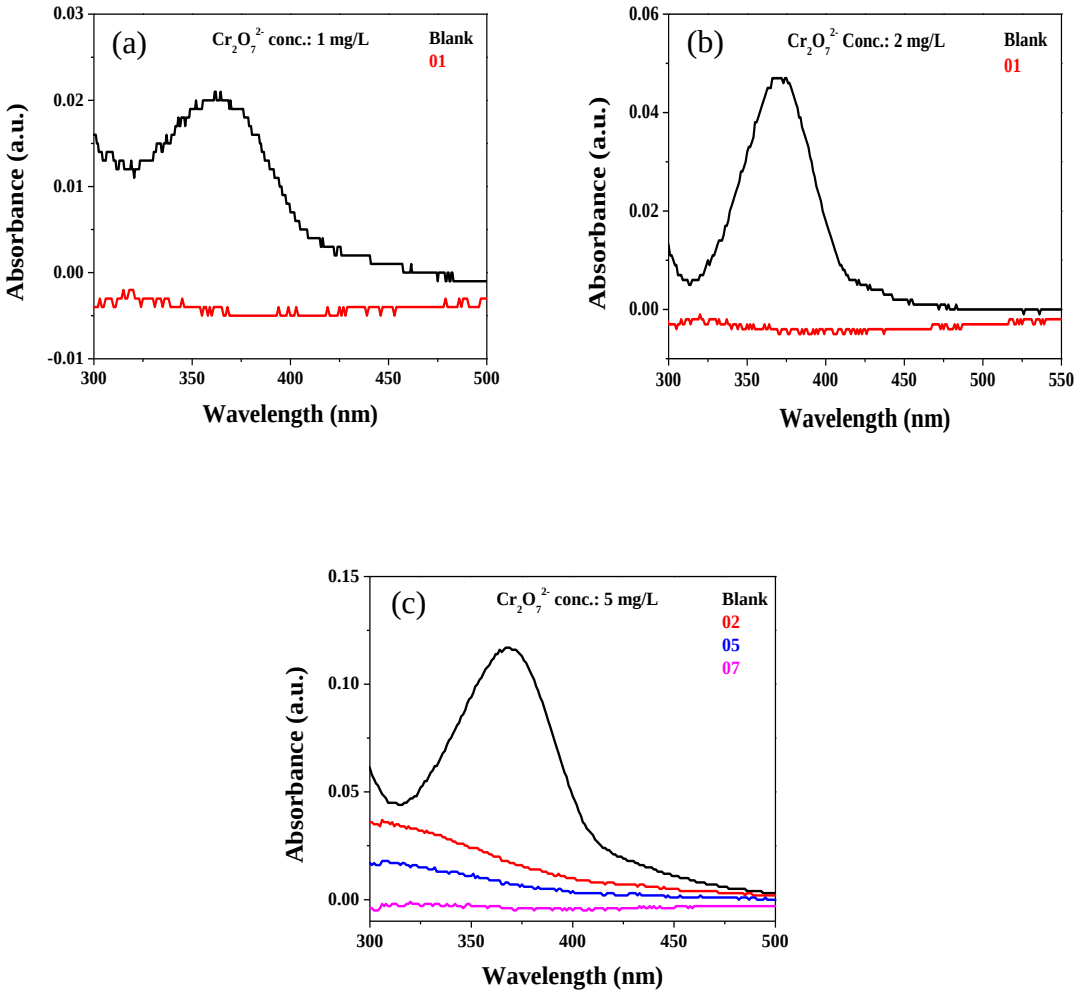

Fig. S18 UV-Vis spectra of adsorption of $Cr_2O_7^{2-}$ at 1 mg/L (a), 2 mg/L (b) and 5 mg/L of solution concentration using ZIS-1.

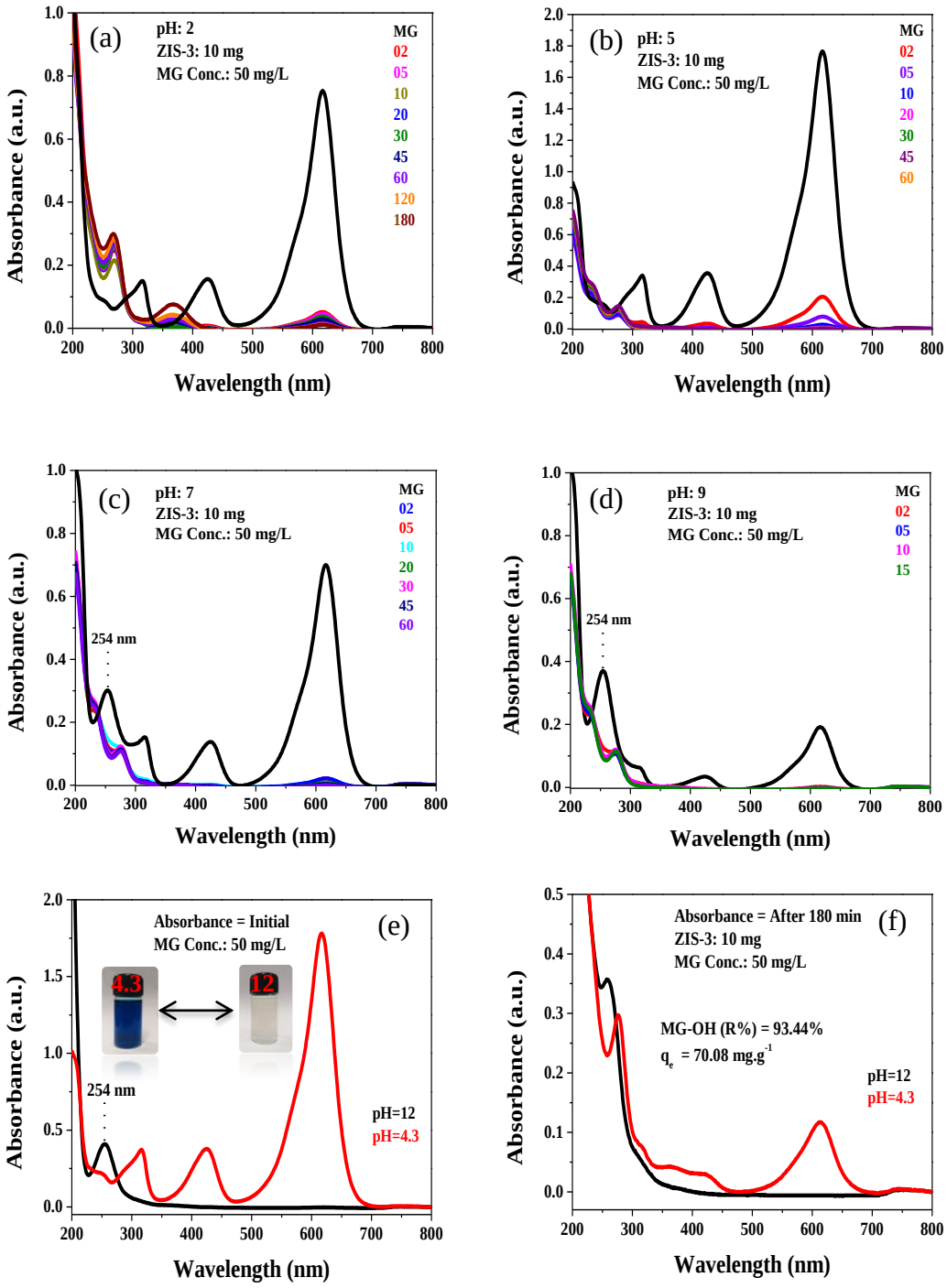

Fig. S19 UV-Vis spectra of MG (50 mg/L) adsorption at pH 2 (a), pH 5 (b), pH 7 (c), pH 9 (d) and initial absorbance of MG at pH 12 and pH 4.3 (e) after adsorption at pH 12 (f) using ZIS-3.

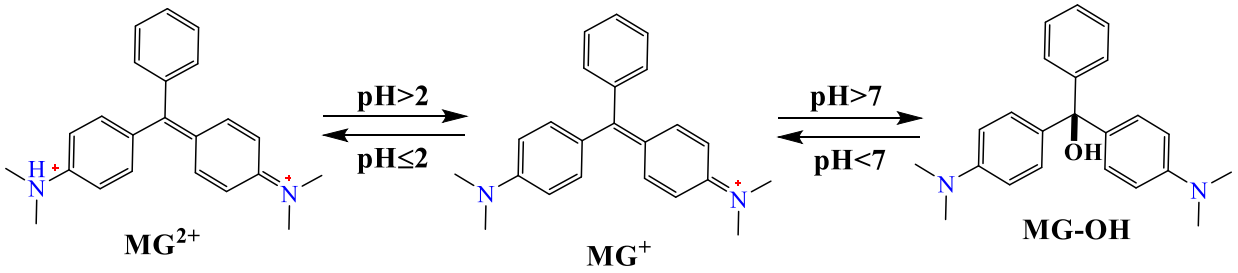

Fig. S20 Three form malachite green dye at different pH; malachite green ion (MG^{+}), Malachite green carbinol (MG-OH) and Protonated MG^{+} (MG^{2+}).

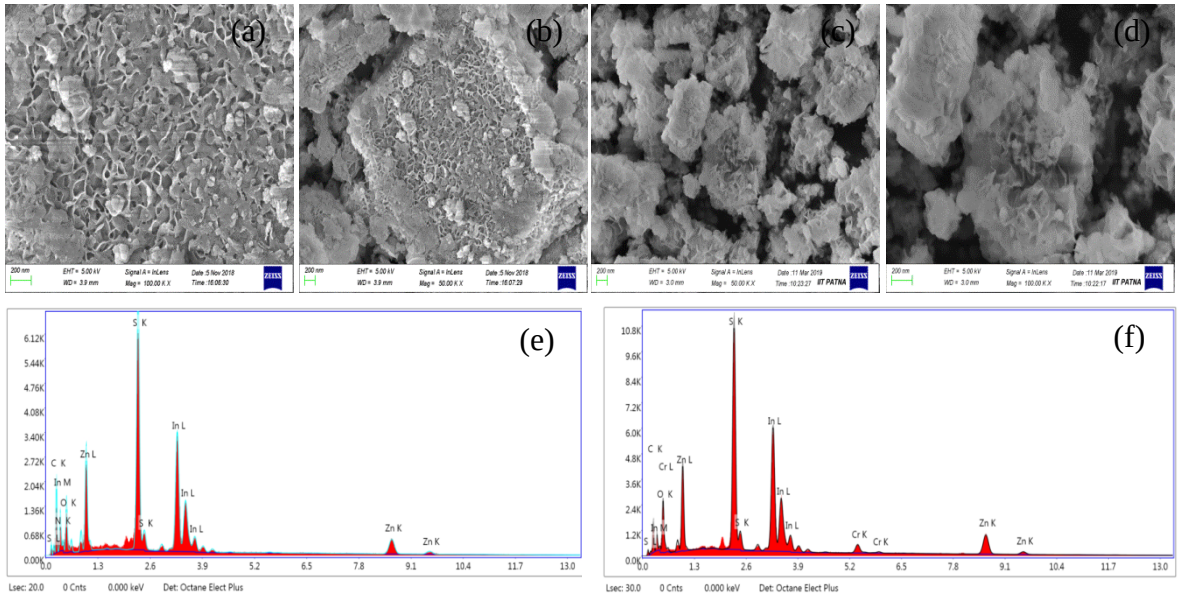

Fig. S21 FE-SEM micrograph of ZIS-3: (a-b) after MG adsorption, (c-d) after $Cr_2O_7^{2-}$ adsorption; EDS line mapping of ZIS-3: (e) after MG adsorption, (f) after $Cr_2O_7^{2-}$ adsorption.

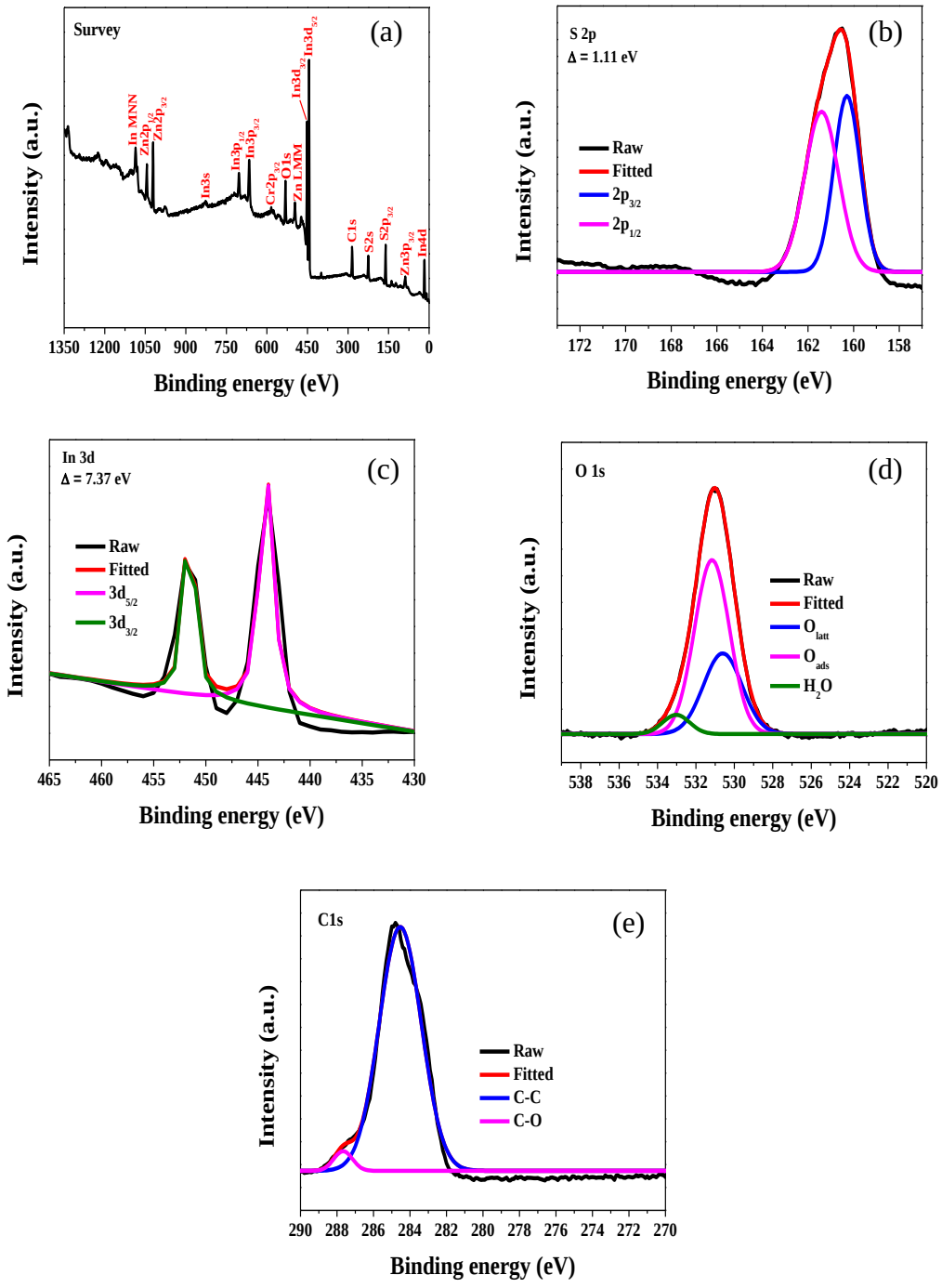

Fig. S22 XPS spectra of ZIS-3 after $Cr_2O_7^{2-}$ adsorption; survey spectra (a), core-level S 2p spectra (b), core-level In3d spectra (c), core-level O1s spectra (d) and core-level C 1s spectra (e).

References

1. M. Yu, Y. Han, J. Li, L. Wang, *Chem. Eng. J.*, 2017, **317,** 493−502.
2. K. Gupta and O. P. Khatri, *Journal of Colloid and Interface Science*, 2017, **501,** 11–21.
3. D. Das and A. Pal, *Chemical Engineering Journal*, 2016, **290,** 371–380.
4. G. Xiong, B.B. Wang, L.X. You, B.Y. Ren, Y.K. He, F. Ding, L. Dragutan, V. Dragutan and Y.G. Sun. *J. Mater. Chem. A*, 2019, **7,** 393-404.
5. P.Zhang, D.Hou, D.O'Connor,X. Li, S. Pehkonen, R.S. Varma, X. Wang, *ACS Sustainable Chem. Eng.*, 2018, **6,** 9229−9236.
6. Liu, H.; Mo, Z.; Li, L.; Chen, F.; Wu, Q.; Qi, L. *J. Chem. Eng. Data*, 2017, **62,** 3036−3042.
7. S. H. Mousavi, F. Shokoofehpoor, A. Mohammadi, *J. Chem. Eng. Data*, 2019, **64,** 135-149.
8. S. Das, S. K. Dash and K. M. Parida, *ASC Omega*, 2018, **3,** 2532-2545.
9. F. Zhang, X. Tang, Y. Huang, A. A. Keller and J. Lan, *Water research*, 2019, **150,** 442-451.
10. E. Solaymani, M. Ghaedi, H. Karimi, M. H. A. Azqhandi and A. Asfaram, *Appl Organometal Chem*. 2017, e3857.
11. F. Guo, X. Jiang, X. Li, X. Jia, S. Liang and L. Qian, *Materials Chemistry and Physics*, 2020, **240,** 122240.
12. E. Mkrtchyan, A. Burakov and I. Burakova, *Materials Today: Proceedings*, 2019, **11,** 404-409.
13. Y. Yu, Y. Li, Y. Wang and B. Zou, *Langmuir*, 2018, **34,** 9359-9365.
14. J. Zhu, H. Gu, J. Guo, M. Chen, H. Wei, Z. Luo, H. A. Colorado, N. Yerra, D. Ding, T. C. Ho, N. Haldolaarachchige, J. Hopper, D. P. Young, Z. Guo and S. Wei, *J. Mater. Chem. A*, 2014, **2**, 2256-2265.
15. Z. Yu, X. Gao, Y. Yao, X. Zhang, G.-Q. Bian, W. D. Wu, X. D. Chen, W. Li, C. Selomulya, Z. Wu and D. Zhao, *Journal of Materials Chemistry A*, 2018, **6**, 3954-3966.
16. Z.-H. Ruan, J.-H. Wu, J.-F. Huang, Z.-T. Lin, Y.-F. Li, Y.-L. Liu, P.-Y. Cao, Y.-P. Fang, J. Xie and G.-B. Jiang, *J. Mater. Chem. A*, 2015, **3**, 4595-4603.
17. S. K. Sahoo and G. Hota, *ACS Applied Nano Materials*, 2019, **2**, 983-996.
18. Y. Cui, J. D. Atkinson, *Chemosphere,* 2019, **228,** 694-701.

19. W. Shen, Y. Mu, T. Xiao and Z. Ai, *Chemical Engineering Journal*, 2016, **285**, 57-68.
20. M. Gheju, I. Balcu and G. Mosoarca, *J Hazard Mater*, 2016, **310**, 270-277.
21. M. A. Behnajady and S. Bimeghdar, *Chemical Engineering Journal*, 2014, **239**, 105-113.
22. T. He, Y. Z. Zhang, X. J. Kong, J. Yu, X. L. Lv, Y. Wu, Z. J. Guo and J. R. Li, *ACS Appl Mater Interfaces*, 2018, **10**, 16650-16659.
23. Z. J. Li, H. D. Xue, Y. X. Ma, Q. Zhang, Y. C. Li, M. Xie, H. L. Qi and X. D. Zheng, *ACS Appl Mater Interfaces*, 2019, DOI: 10.1021/acsami.9b17074.
24. Y. Wei, W. Huang, Y. Zhou, S. Zhang, D. Hua and X. Zhu, *Int J Biol Macromol*, 2013, **62**, 365-369.